Effect of Nano-Textured Silicon Substrate on the Synthesize of Metal Oxides Nanostructures

Fatemeh Sheikhshoaei[1], Mahdiyeh Mehran[1*] and Iran Sheikhshoaie[2]

[1]RF MEMS and Bio-Nano Electronics Lab, Department of Electrical Engineering, Shahid Bahonar University of Kerman, Kerman, Iran.
[2]Department of Chemistry, Faculty of Sciences, Shahid Bahonar University of Kerman, Kerman, Iran.

(*) Corresponding author: m.mehran@uk.ac.ir

Abstract

Metal oxides such as ZnO, SnO_2 and W_2O_3 with super properties are widely used in the different fields of science and proper synthesis of these materials is of the great importance. In this work, some metal oxides with nano structures including SnO_2 nanopyramids, V_2O_5 nanowires and hierarchical structure of SnO_2 nanopyramids and ZnO nanowires were grown at low temperature by hydrothermal method. Both bare and nano-textured silicon substrates were employed for the synthesis of mentioned nano structures. Nanotextures of silicon substrate are called nano-grasses and were obtained by a deep reactive ion etching (DRIE) method with successive etching and passivation sub-cycles, using an RF-plasma at different conditions. Comparing SEM images of the synthesized nanostructures on two simple and nanotextured silicon substrates show that there are great differences between growths on these substrates such as higher density and better uniformity. Therefore, application of nano-textured silicon substrates can improve the growth process of metal oxide nanostructures, which can promote various applications of these materials in the different scientific fields.

Keywords: *SnO_2, V_2O_5, Nanostructure, Hydrothermal, RIE, Silicon nanograss.*

1. INRODUCTION

Binary metal oxides have super properties and nowadays are widely used as transparent conducting oxides, lithium-ion batteries, gas sensors, supercapacitors and dye sensitized solar cells. Some of these metal oxides are ZnO, SnO_2, W_2O_3, V_2O_5 and In_2O_3 [1].

Physical, chemical and biological properties of materials at the nanoscale are very different from the bulk of them [2]. For example, various quantum mechanical effects are observed, such as the increase in the energy gap of a semiconducting material with reduction in size [3]. These properties enable manufacturing complex and multifunctional materials which have great potential in the improving many aspects of our life. Recently, there are growing interest in the one-dimensional nanomaterials such as nanorods, nanowires, nanofibers and nanotubes of various metal oxides [2]. Nanowires have unique properties that arise from their low dimensions and high surface to volume ratio of them. Chemical species that adsorb on the nanowire surfaces, strongly affects their electrical conduction, therefore extremely efficient chemical and biological sensors can be developed. Other applications of metal oxides are in the optoelectronic devices, solar energy conversion, photoelectrochemical cells and heterogeneous photocatalysis [4]. Pyramidal nanostructures on a substrate can increase its surface and functionality in comparison with the flat one. This improved substrate, can be used for the subsequent growth procedures.

One of the metal oxides that receives significant attention these days is vanadium oxide and its compounds. This is because of their structural versatility combined with their unique chemical and physical properties. Vanadium oxide compounds have prominent properties and potential applications such as catalysts, chemical sensors, high-energy density lithium-ion batteries, electrochemical and optical devices [5, 6].

Because of these potentials, a wide range of V_2O_5 nanostructures has been synthesized to improve electrochemical properties before, such as nanowires, nanospheres, nanoribbons, nanosheets and nanobelts [7]. Researchers explored numerous methods toward synthesizing V_2O_5 nanostructures such as chemical vapor deposition (CVD), template assisted [8], reverse micelle synthesis, electrospinning, thermal evaporation and microwave [6]. Other approaches for synthesizing V_2O_5 nanowires are hydrothermal/solvothermal, sol–gel and electrodeposition [9]. Meanwhile, proper synthesis of V_2O_5 is quite essential.

Another metal oxide that is one of the smart materials due to its good stability, non toxicity and low cost is tin dioxide. It is n-type semiconductor with a wide-bandgap of 3.6 eV [1], large exciton binding energy, high electrical conductivity, high optical transparency and small exciton Bohr radius. SnO_2 film is a good candidate to be used in solar cells, gas sensors and lithium batteries [10]. Some of its potential applications are in photocatalysis, far-infrared detectors, optoelectronic devices, catalyst supports, antireflective coatings and transparent electrodes. Several methods have been used to prepare SnO_2 nanostructured films such as sol-gel, spray pyrolysis deposition (SPD), chemical vapor deposition (CVD), sputtering, hydrothermal [10] and evaporation of elemental tin in an oxygen atmosphere [4]. Anyway, proper synthesis of SnO_2 for different applications is quite important.

ZnO is a II–VI compound semiconductor [11], which gets lots of attention because of non toxicity, low cost and having good properties for a wide range of applications, such as photonics because of its wide bandgap of 3.37 eV and high exciton binding energy of 60 meV. Other applications of ZnO are transparent high power electronics, optical waveguides, piezoelectric converters, gas-sensors, window materials for display, solar cells, etc [12]. Properties and applications of ZnO crucially depend on its morphology, size and orientation. Therefore, controllable synthesis of the ZnO nanostructures is important. ZnO nanostructures have been synthesized by various physical and chemical methods such as vapor–liquid–solid, molecular beam epitaxy and solution processes [13] such as chemical precipitation, sol-gel and solvothermal/hydrothermal reaction [14]. Among all, room temperature solution ways such as hydrothermal are particularly attractive because they are simple, low-temperature and catalyst-free process and there is no limitation for their substrate. Moreover, morphology of the nanostructures can be tuned effectively by changing synthesis parameters [13]. Vertically aligned one-dimensional nanowires can provide an interesting solution to achieve ultrahigh-density advanced nanoscale devices [15]. These devices increase effective surface and can be used as high sensitive electronic and photonic devices [16], gas and bio-sensors. In this paper, effects of substrate morphology on the formation of metal oxide nanostructes were examined. Simple and nano grass silicon substrates were employed for the synthesis of V_2O_5, SnO_2 and ZnO nano structures. The consequence of silicon grass formation is great increase in the effective surface of the substrate, which can be used for physical, electrical and chemical applications [17] such as gas and bio-sensors, ion-selective field effect transistors, microelectromechanical systems, solar cells [18], superhydrophobic

and hydrophilic surfaces. A modified RIE process were employ for the incorporation of nano grasses to the silicon substrate [17]. Employed RIE process is sequential like Bosch process [18-21].

This paper is organized as follows: in the section 2 synthesis and fabrication methods are proposed. Next in the section 3, different results of the prepared samples such as SEM images, EDS and XRD are presented and at last, this paper terminates with the conclusion.

2. MANUFACTURING AND SYNTHESIS METHOD

In this study SnO_2 nanopyramids, V_2O_5 and ZnO nanowires have been grown on both simple and nano-textured silicon substrates. A modified RIE process is applied to the silicon substrate for the incorporation of nano-textures or nano-grasses to it.

2.1. Silicon Nano-Grass Formation

In this study, two simple and nano-grass silicon substrates were employ for the synthesis of different metal oxide nanostructures. After cleaning silicon substrates using RCA#1 solution ($NH_4OH:H_2O_2:H_2O$, 1:1:5), they blow dried. Silicon nano-grasses were incorporated to one of substrates employing a modified DRIE process which is reported elsewhere [18-21] as it is shown in the figure 1. This RIE process consists of successive steps of passivation and etching sub-cycles like Bosch process [22]. Passivation sub-cycle is done in the presence of a gas mixture of O_2, H_2 and SF_6 with the proper plasma condition while etching sub-cycle is performed in the presence of SF_6 with suitable plasma condition. Grass formation could be considered as one of the undesirable side effects of DRIE in the evolution of high aspect ratio features. The vertical etching process, however, can be adjusted to obtain grass-free structures at both micro and nanoscales with high aspect ratios. On the other hand, by using proper flows of gases

during passivation and etching sub-cycles, one can manipulate vertical or spaghetti-like Si nano-grasses with a height of 2-3 μm and width of 30 to 100 nm with the aspect ratios of the order 50. Figure 2 shows schematic of grass formation process. For such structures, in the passivation step, a mixture of H_2/O_2 gases with typical flows of 100 and 85 sccm and a trace value of SF_6 was used, whereas for the etching step, SF_6 was used as the inlet gas with typical flows of 10–40 sccm. Plasma power and duration of the passivation sub-cycle were set at 150 W and 50 seconds and for the etching sub-cycle 130 W and 10 seconds respectively [18-21]. In the next step, a thermal oxide with a thickness of 0.1 μm was grown on both simple and silicon nano-grass substrates.
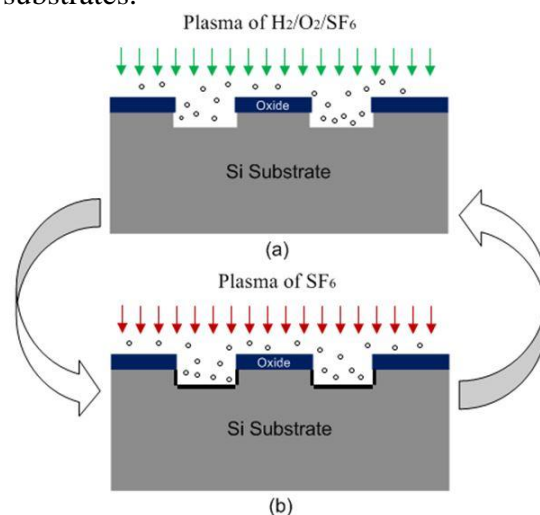

Figure 1. *Different sub-cycles of DRIE process, (a) passivation and (b) etching. These sub-cycles could be repeated several times as necessary [22].*

2.2. Synthesis of SnO₂ Nanopyramids

SnO_2 nanopyramids were synthesized using hydrothermal method. Before employing this method, a seed layer was deposited on the substrate which could improve latter growing of nanostructures. Seed layer was prepared using stannic acid gel ($SnO_2.nH_2O$) which was obtained by adding a $SnCl_4.5H_2O$ solution to $NaHCO_3$ solution (1:1) in a drop-wise manner. Then, obtained white precipitate was collected and washed with sufficient

amount of deionized water to remove chloride ions. Subsequently, this precipitates were dispersed in distilled water and adjusted pH of the solution to 10.5 with ammonium hydroxide [22]. Afterward this solution spin coated 4 times on nano-grass silicon substrate and after each step substrate dried at 60-70°C. At last, annealing was done at 450°C for an hour.
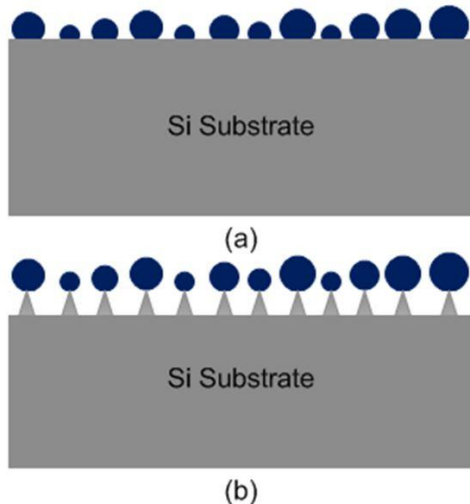

Figure 2. *(a) Remained protective layer on the silicon substrate after passivation sub-cycle and (b) Remained protective layer behaves as a mask in the etching sub-cycle and protects silicon beneath so grasses form [18-21].*

Another method for creating sol-gel for spin coating is preparing a mixture of $SnCl_2.2H_2O$ (0.05 M) in 10 ml of absolute ethanol. After preparing this mixture, it was stirred on a hot plate at 40-50°C for 10-30 min. This process was done for creating a seed layer of simple substrate and after spin coating of the gel, annealing was done for 2 hours. SnO_2 nanopyramids were synthesized using hydrothermal method with a mixture of 4 ml $SnCl_4.5H_2O$ (0.5 M), 10 ml NaOH (5 M) and 80 ml ethanol/water solution. Then, this solution was stirred for 10 min [23]. After preparing solution, the above mentioned samples were floated and kept in it for 15 hours at 90°C.

2.3. V_2O_5 Nanowires Growth

In the first step, V_2O_5 seed layers were prepared by spin-coating seed solution on the Si substrates, followed by a thermal annealing treatment. For it, 6 mmol ammonium metavanadate (NH_4VO_3) was dissolved in 30 ml deionized water at 50 ºC and stirred magnetically. Then nitric acid was added drop-wise to form an orange solution with a pH value of 2.1–2.5, which was served as the seed solution. Then the seed solution spin-coated on the simple and nano-grass silicon substrates with spinning speed of 1500 rpm for 30 sec. After that, substrates were baked for 10 min at 80 °C on a hot plate. Spin-coating and baking procedures were repeated six times to guarantee an adequate coverage of the V_2O_5 seeds on the substrates. After spin-coating, annealing was done to transform the precursor into V_2O_5 seed particles and to guarantee good adhesion between seeds and substrate [24]. Finally, obtained substrates were annealed at 600 ºC in the air pressure for 2 h. For growing nanowires, NH_4VO_3 was used as vanadium source again. The peroxovanadate were prepared by dissolving 0.004 mol NH_4VO_3 in 40mL of H_2O and C_2H_5OH solution. Then HNO_3 was added to the solvent to adjust the pH of the solution to 3–4. Mixture ultrasonically mixed at room temperature for 15 min and then samples were placed in this solution and kept at 130 ºC for 2 h [8].

2.4. ZnO Nanowires Growth

For growth of ZnO nanowires, ZnO seed layer was prepared followed by the hydrothermal synthesis process. Seed layer was prepared with dissolving zinc acetate dihydrate ($Zn(CH_3COO)_2.2H_2O$) in the ethanol with concentration of 0.05 M. Then, solution was stirred at 60°C for 10-30 min to yield a clear and homogeneous solution [14]. In the next step, solution were spin coated on the Si substrates. Spin coating of the substrates were done with speed of 2500 rpm for 10 Sec and repeated

Sheikhshoaei, Mehran and Sheikhshoaei

4 times for better uniformity of the attained seed layer. Finally, the substrates were annealed at 450°C for an hour to achieve ZnO seed layers. ZnO nanowires were synthesized hydrothermally at 90 °C. For this synthesis, $C_6H_{12}N_4$ (HMT) and $Zn(NO_3)_2.6H_2O$ with concentrations of 0.035 M were dissolved in 50 mL of DI water, then the substrates were placed in the solution and heated at 90 °C for 4 hours in an oven. Finally, samples with ZnO nanowires were washed thoroughly with DI water and blow dried [13].

For hierarchical structure of SnO_2 nanopyramids and ZnO nanowires, depicted process in sections 2.2 and 2.3 were employed to the simple and nano-grass silicon substrates respectively. At last, sintering was done for 1 h at 400 °C.

3. RESULT AND DISCUSSION

SEM image of a silicon nano-grass substrate is shown in figure 3. In comparison with a simple silicon substrate, effective surface area is highly increased.
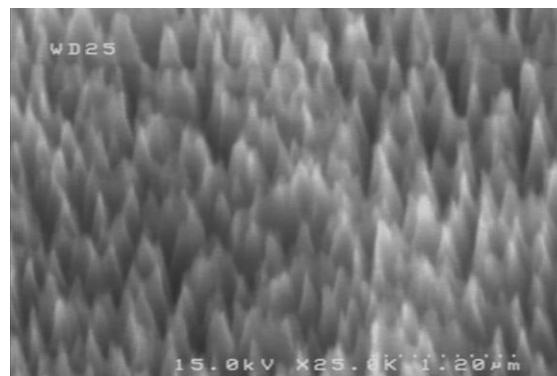

Figure 3. SEM image of nano-grass silicon substrate.

Figure 4 shows SEM images of the synthesized SnO_2 nanostructures on two different silicon substrates. It is obvious that these nanostructures are pyramid shape. Part (a) of this figure shows synthesized SnO_2 nanopyramids on silicon nano-grass substrate, while part (b) shows these textures on the simple silicon substrate.
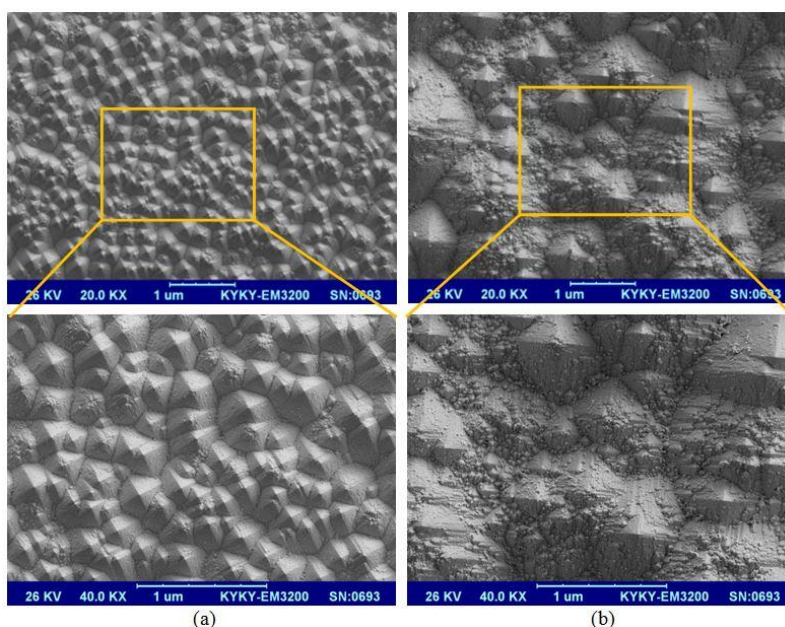

(a)   (b)

Figure 4. SEM images of synthesized SnO_2 nanopyramids, (a) on a nano-grass silicon substrate and (b) on a simple silicon substrate.

As it is observed in parts of figure 4, growth of SnO_2 nanopyramids on a nanostructured silicon substrate is better and more regular. It can be seen in part (a) of this figure, apex of nanopyramids is sharper. There are some other nanostructures on each pyramid face, which promotes the performance and the effective surface area of the substrate drastically. In part (b) of figure 4,

formation of nanopyramids is very irregular and is similar to a destroyed region. Therefore, application of a nanostructured base, like silicon nano-grass substrate, promotes morphology of the created nanostructures on it and this improves various applications of this material in different science fields.

Figure 5 shows SEM images of the synthesized V_2O_5 nanowires on the simple and nano-grass silicon substrates. These nanowires are with height of 1-2 μm and a width under 100 nm.
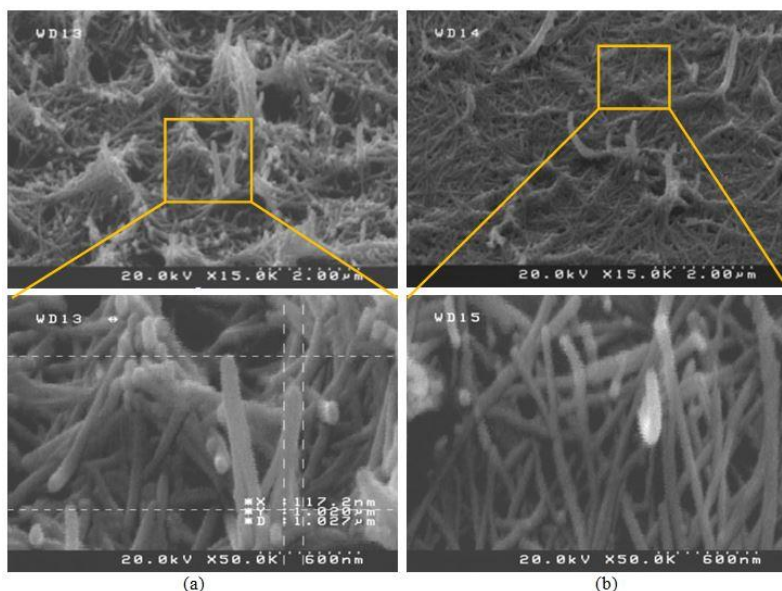

Figure 5. *SEM images of V_2O_5 nanowires, (a) on a nano-grass silicon substrate and (b) on a simple silicon substrate.*

As it is obvious in the figure 5, density of grown nanowires on the nano-textured silicon substrate is different from simple one so, the effective surface area of the synrhesized nano wires could be greatly enhanced by using such a nano-textured substrate. Another issue is number of vertically aligned V_2O_5 nanowires which have been increased on the nano-textured substrate. This can be attributed to the nano-grasses of the substrate which help better alignment of the nanowires. However seed layer that was used before synthesizing V_2O_5 nanowires, couldn't stay horizontally on a bare or simple substrate and all of them laid down. In the previous works [9, 25], V_2O_5 nanowires aren't grown vertically by hydrothermal method because of easily self-aggregation [25], however in this work the ratio of aligned nanowires could be increased because of the nanotextured substrate.

Also the effect of nano-textured substrate on the synthesis of hierarchical structures were surveyed, which has been demonstrated in the section 2.4. SnO_2 nanopyramids were grown on both simple and nano-grass silicon substrates and in the next step, ZnO nanowires were synthesized on the SnO_2 pyramids. SEM images of these samples can be observed in the figure 6.

As it is shown in the figure 4 that synthesis of SnO_2 nanopyramids on the simple silicon substrate is irregular while surface of the formed pyramids is nanotextured. Grown ZnO nanowires on such a nano-textured substrate are longer and a dense network of nanowires are formed which is obvious in the figure 6. This can be attributed to the nano-textures of irregular SnO_2 pyramids that behave like defect sites and help growth of ZnO nanowires. Similar to the previous results, growth on the nano-textured substrates is denser and more regular.
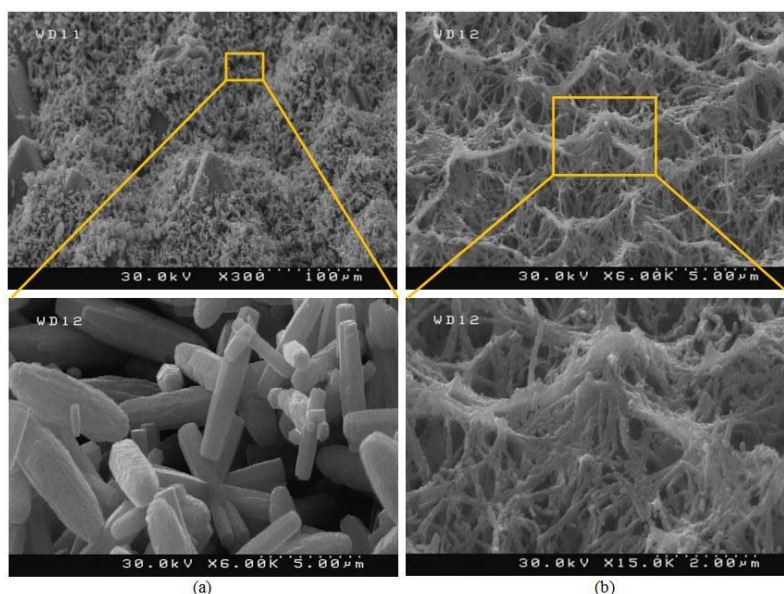
Figure 6. *SEM images of hierarchical structure of SnO₂ pyramids and ZnO nanowires on, (a) nano-grass silicon substrate and (b) simple substrate.*

The crystallographic structure information about the hierarchical SnO_2-ZnO structure is characterized by X-ray diffractometry (XRD) as is shown in figure 7. The main diffraction peaks are at 28.952, 31.448, 35.404, 35.950, 38.886, 42.621, 47.019, 47.907, 56.798 and 64.012 degrees, which correspond to SiO_2, SnO_2 and ZnO as it is shown in the figure 7. The crystal structure of SiO_2 is tetragonal with a lattice constants of $a = 10.24$ Å, $b = 10.24$ Å and $c = 34.38$ Å which is based on the reference code 00-040-1498. For SnO_2 crystal structure peaks are accrued in (110), (101), (210), (221), (301) and (320) crystal planes which confirms the tetragonal crystal structure of the as-synthesized SnO_2 with lattice constants of $a = 4.74$ Å, $b = 4.74$ Å and $c = 3.19$ Å based on the reference code of 00-041-1445. Related peaks to ZnO crystal structure are for (100), (002), (101), (102), (110), (103), (112), (201), (004) and (202) crystal planes which confirms crystal structure of hexagonal with $a = 3.25$ Å, $b = 3.25$ Å and $c = 5.21$ Å as lattice constants according to reference code of 00-036-1451.

Finally, using Debye-Scherrer equation, which is shown in equation 1, and FWHM from XRD pattern [26], crystal size of SnO_2 and ZnO are calculated. For SnO_2, sizes change from 12.97 nm to 39.89 nm with an average of 23.91 nm while for ZnO, sizes change between 13.18 nm and 41.92 nm with an average of 24.51 nm.

$$D_{hkl} = K\lambda/(B_{hkl}\cos\theta) \qquad (1)$$

In Equation 1, D_{hkl} is the crystalline size in the direction perpendicular to the lattice planes, hkl are the Miller indices of the planes that has been analyzed, K is a numerical factor that often mentions as the crystalline-shape and normally equals to 0.9, λ is the wavelength of the X-rays, B_{hkl} is the width (full-width at half-maximum) of the X-ray diffraction peak (radian) and θ is the Bragg angle [26].

Results of Energy-Dispersive X-ray Spectroscopy (EDS) measurements for the hierarchical SnO_2-ZnO structure are shown in Fig. 8. This analyze again confirms existence of Zn, O, Sn and Si with weight percentage of 53.91%, 15.9%, 0.14% and 2.34% respectively. Therefore, as-synthesized nanostructures do not have impurity. Some other peaks that are observed in the analysis figure are created at characterization stage.
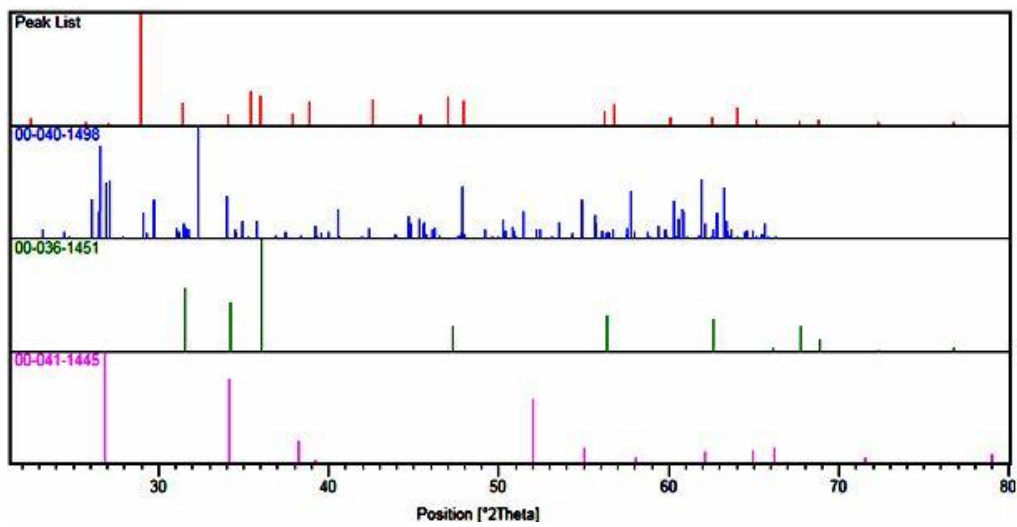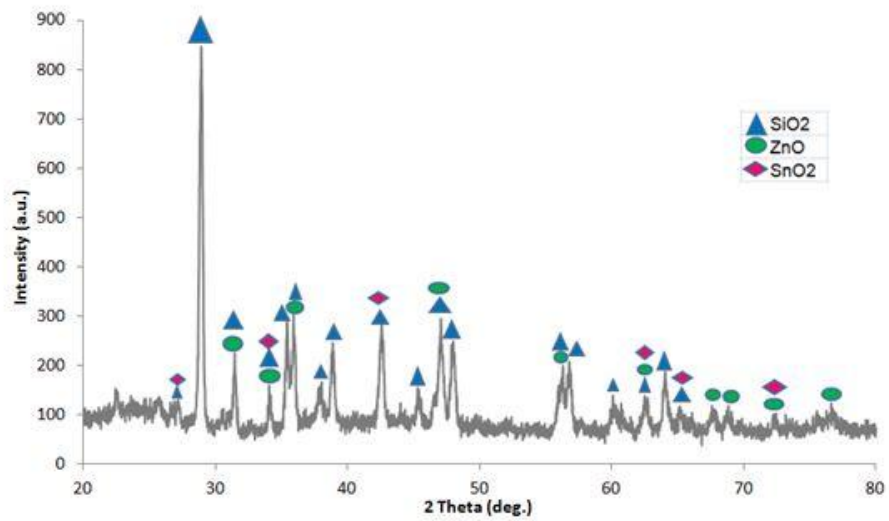
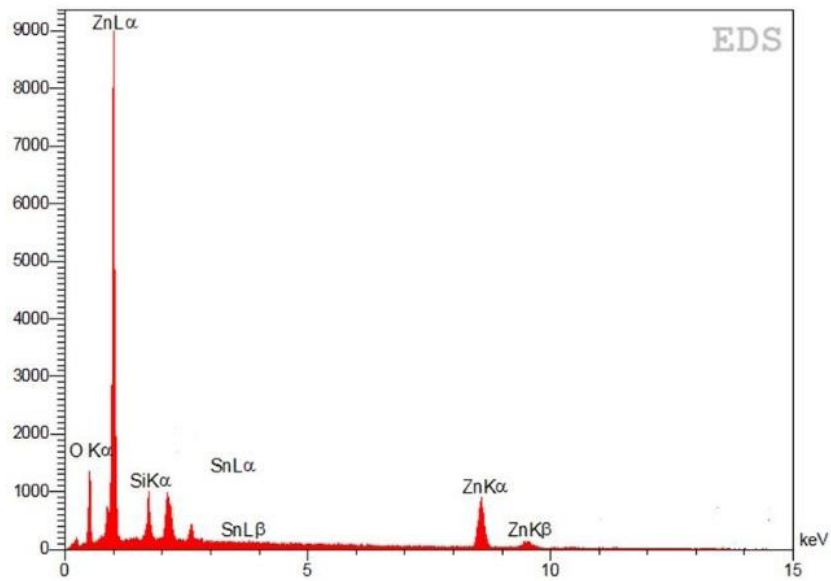**Figure 7.** XRD patterns of the hierarchical SnO$_2$-ZnO structure on simple and nano-grass silicon substrate.

Figure 8. EDS measurement of hierarchical SnO$_2$-ZnO structure on simple and nano-grass silicon substrate.

Sheikhshoaei, Mehran and Sheikhshoaei

4. CONCLUSIONS

Several metal oxides on two types of simple and nano-grass silicon substrates were successfully synthesized using hydrothermal method. Plasma etching of silicon with two successive sub-cycles of passivation and etching was utilized for the evolution of nano-grasses on the silicon substrate. Comparing SEM images of the obtained results indicate that growth on the silicon nano-grass substrate is uniform and better. It seems that defects which are formed during nano-grass configuration on the silicon substrate, decrease mismatch between silicon and metal oxide lattice, therefore formation of the primary seed layer improves which leads to the more uniform growth. For the high-quality growth of metal oxide nanostructures, silicon nano-textured substrates are good options to achieve this goal.

REFERENCES

1. Kuang, X., Liu, T., Wang, W., Hussain, Sh., Peng, X. (2015). "Controlled synthesis of SnO_2 hierarchical architectures made of ultrathin nanoflakes for enhanced ethanol gas sensing properties", *Applied Surface Science*, 351: 1087–1093.
2. Aluri, G. S. (2012). "*Highly Sensitive and Selective Chemical/Gas Sensors Using Hybrid Nanowire and Nanocluster Based Devices*", Ph.D Thesis of George Mason University.
3. Najafi, M., Haratizadeh, H. (2015). "Synthesize and optical properties of ZnO: Eu microspheres based nano-sheets at direct and Indirect excitation", *Int. J. Nanosci. Nanotechnol.*, 11(2): 101-113.
4. Wang, W., Xu, C., Wang, X., Liu, Yi., Zhan, Y., Zheng, Ch., Song, F., Wang, G. (2002). "Preparation of SnO_2 nanorods by annealing SnO_2 powder in NaCl flux", *Journal of Materials Chemistry*, 12: 1922–1925.
5. Wang, Ch., Yin, L., Zhang, L., Xiang, D., Gao, R. (2010). "Metal Oxide Gas Sensors: Sensitivity and Influencing Factors", *Sensors*, 10: 2088-2106.
6. Zhou, F., Zhao, X., Liu, Y., Yuan, C., Li, L. (2008). "Synthesis of Millimeter-Range Orthorhombic V_2O_5 Nanowires and Impact of Thermodynamic and Kinetic Properties of the Oxidant on the Synthetic Process", *European Journal of Inorganic Chemistry*, 16: 2506–2509.
7. Steunou, N., Livage, J. (2015). "Rational design of one-dimensional vanadium (V) oxide nanocrystals: an insight into the physicochemical parameters controlling the crystal structure, morphology and size of particles", *Cryst. Eng. Comm.*, 17: 6780-6795.
8. Mu, J., Wang, J., Hao, J., Cao, P., Shuoqing, Zh., Wen, Z., Bin, M., Sibo, X. (2015). "Hydrothermal synthesis and electrochemical properties of V_2O_5 nanomaterials with different dimensions", *Ceramics International*, 41: 12626–12632.
9. Mai, L., Xu, X., Xu, L., Han, C., Luo, Y. (2011). "Vanadium oxide nanowires for Li-ion batteries", *Journal of Materials Research*, 26(17): 2175-2185.
10. Zhai, T., Liu, H., Li, H., Fang, X., Liao, M., Li, L., Zhou, H., Koide, Y., Bando, Y., Golberg, D. (2010). "Centimeter-Long V_2O_5 Nanowires: From Synthesis to Field-Emission, Electrochemical, Electrical Transport and Photoconductive Properties", *Advanced Materials*, 22: 2547–2552.
11. Boroojerdian, P. (2013). "Microwave–assisted hydrothermal synthesis and optical characterization of SnO_2 nanoparticles", *Int. J. Nanosci. Nanotechnol.*, 9(3): 139-142.
12. Lamba, R., Umar, A., Mehta, S.K., Kansal, S. K. (2015). "ZnO doped SnO_2 nanoparticles heterojunction photo-catalyst for environmental remediation", *Journal of Alloys and Compounds*, 653: 327-333.
13. Chitanu, E., Ionita, Gh. (2012). "HYDROTHERMAL GROWTH OF ZNO NANOWIRES", *the Scientific Bulletin of VALAHIA University - MATERIALS and MECHANICS*, 7: 9-13.
14. Dong, J. J., Zhen, Ch. Y., Hao, H.Y., Xing, J., Zhang, Z. L., Zheng, Z. Y., Zhang, X. W. (2013). "Controllable synthesis of ZnO nanostructures on the Si substrate by a hydrothermal route", *Nanoscale Research Letters*, 8: 378-384.
15. Nguyen, Ph., Ng, H. T., Yamada, T., Smith, M. K., Li, J., Han, J., Meyyappan, M. (2004). "Direct Integration of Metal Oxide Nanowire in Vertical Field-Effect Transistor", *NANOLETTERS*, 4: 651-657.
16. Velazquez, J. M., Banerjee, S. (2009). "Catalytic Growth of Single-Crystalline V_2O_5 Nanowire Arrays", *small*, 5: 1025–1029.
17. Aneesh, P. M., Vanaja, K. A., Jayaraj, M. (2007). "Synthesis of ZnO nanoparticles by hydrothermal method", *Nanophotonic Materials IV, Proceedings of SPIE*, 6639: 1-9.

18. Mehran, M., Sanaee, Z., Mohajer Zadeh, S. Sh. (2010). "Formation of silicon nanograss and microstructures on silicon using deep reactive ion etching", *Micro & Nano Letters*, 5: 374–378.
19. Mehran, M., Mohajer Zadeh, S. Sh., Sanaee, Z., Abdi, Y. (2010). "Nanograss and nanostructure formation on silicon using a modified deep reactive ion etching", *APPLIED PHYSICS LETTERS*, 96: 1-3.
20. Mehran, M., Sanaee, Z., Abdolahad, M., Mohajer Zadeh, S. Sh. (2011). "Controllable silicon nanograss formation using a hydrogenation assisted deep reactive ion etching", *Materials Science in Semiconductor Processing*, 14: 199–206.
21. Mehran, M., Kolahdouz, Z., Sanaee, Z., Azimi, S., Mohajer Zadeh, S. Sh. (2011). "Evolution of high aspect ratio and nanograss structures using a modified low plasma density reactive ion etching", *The European Physical Journal Applied Physics*, 55: 11302-11310.
22. Sammak, A., Azimi, S., Izadi, N., Khadem Hosseini, B., Mohajer Zadeh, S. Sh. (2007). "Deep Vertical Etching of Silicon Wafers Using a Hydrogenation-Assisted Reactive Ion Etching", *Journal of Microelectromechal Systems*, 16: 912-918.
23. Shi, S., Liu, Y., Chen, Y., Zhang, J., Wang, Y., Wang, T. (2009). "Ultrahigh ethanol response of SnO_2 nanorods at low working temperature arising from La_2O_3 loading", *Sensors and Actuators B*, 140: 426–431.
24. Qin, Y., Fan, G., Liu, K., Hu, M. (2014). "Vanadium pentoxide hierarchical structure networks for high performance ethanol gas sensor with dual working temperature characteristic", *Sensors and Actuators B: Chemical*, 190: 141-148.
25. Mai, L., Xu, L., Han, C., Xu, X., Luo, Y., Zhao, S., Zhao, Y. (2010). "Electrospun Ultralong Hierarchical Vanadium Oxide Nanowires with High Performance for Lithium Ion Batteries", *Nanoletter,* 10: 4750–4755.
26. Holzwarth, U., Gibson, N. (2011). "The Scherrer equation versus the 'Debye–Scherrer equation'", *NATURE NANOTECHNOLOGY*, 6: 534.